PRESSURE TRANSIENT ANALYSIS IN SINGLE AND TWO-PHASE WATER BY FINITE DIFFERENCE METHODS

G. F. BERRY, J. G. DALEY

Components Technology Division, Argonne National Laboratory, 9700 South Cass Avenue, Argonne, Illinois 60439, U.S.A.

SUMMARY

An important consideration in the design of LMFBR steam generators is the possibility of leakage from a steam generator water tube. The ensuing sodium/water reaction will be largely controlled by the amount of water available at the leak site, thus analysis methods treating this event must have the capability of accurately modeling pressure transients through all states of water occurring in a steam generator, whether single or two-phase.

The equation systems of the present model consist of the conservation equations together with an equation of state for one-dimensional homogeneous flow. These equations are then solved using finite difference techniques with phase considerations and non-equilibrium effects being treated through the equation of state. Fluid-structure interactions were not included at the time of this writing but are treated in the systems code which will contain this water-side transient model.

The methods of calculating water properties were developed specifically for this work due to the unavailability of computational methods having the necessary precision and using the desired independent variables (specific energy and density) over the required range of property states.

The basis for water property computation is Keenan's "fundamental equation of state" which is applicable to single-phase water at pressures less than 1 000 bars and temperatures less than 1 300°C. This provides formulations allowing computation of any water property to any desired precision. Two-phase properties are constructed from values on the saturation line. The use of formulations permits the direct calculation of any thermodynamic property (or property derivative) to great precision while requiring very little computer storage, but does involve considerable computation time. For this reason an optional calculation scheme based on the method of "transfinite interpolation" is included to give rapid computation in selected regions with decreased precision. This method, simply stated, calculates values within a region based on values at the boundaries of the region. Thus it is necessary only to provide a few one-dimensional curve-fits of properties on region boundaries (cubic splines were found to give excellent results) rather than storing massive two-dimensional arrays of data. The computer storage requirements for approximation using this technique are very small, precision quite good, and closed form solutions are possible for the choice of independent variables.

The conservation equations were solved using the second order Lax-Wendroff scheme which includes wall friction, allows the formation of shocks and locally supersonic flow. Computational boundary conditions were found from a method-of-characteristics solution at the reservoir and receiver ends. The local characteristics were used to interpolate data from inside the pipe to the boundary.

The results obtained using this code show stable solutions reaching steady state from reservoir conditions initially subcooled, superheated or two-phase. Comparisons with experimental data are given as well as comparisons with results obtained from critical flow models and other computational schemes.

Nomenclature

A - pipe area

B - subscript for boundary mesh point

c - fluid wave speed

D - hydraulic diameter

E - Young's modulus

e - internal energy

$\vec{F}$ - flux vector

f - fanning friction factor

g - gravity constant

h - pipe wall thickness

j - cell index

ℓ - length of pipe

$\dot{m}$ - mass addition

P - pressure

$\dot{q}$ - heat flux

R - characteristic point of positive characteristic

S - characteristic point of negative characteristic

$\vec{S}$ - source vector

T - characteristic point of particle path

t - time

u - fluid velocity

$\vec{U}$ - variable vector

v - specific volume

x - water quality

o - subscript for reservoir or stagnation properties

δ - stability reduction factor

ρ - density

θ - angle of elevation

Introduction

The subject of two-phase blowdown has received considerable attention from the nuclear industry due to safety studies of the transient following a hypothetical loss-of-coolant accident in water-cooled reactors. This interest has resulted in the development of thermal/hydraulic analysis codes which model the dynamic response of the primary system to such an event. Much of this experimental and analytical work finds direct application also in modeling the effect of hypothetical leaks in liquid metal fast breeder reactor (LMFBR) secondary systems where the primary interest is the initial hydraulics of the blowdown event.

Here, the concern is with leaks in the steam generator tubes emitting water which will react chemically with the intermediate system coolant (sodium). Although such an event would not involve the release of radioactivity, close attention must be paid to this problem, both to minimize the possibilities of its occurrence as well as to determine the design of structural components, relief system, and safety mechanisms so that the LMFBR secondary system can withstand such an accident with no effect on plant operation other than a temporary partial loss in generating capacity as the affected steam generator system is refitted for service (typical designs call for three independent and identical steam generator systems per reactor).

Blowdown conditions exist following the rupture of one or more water tubes. Knowledge of the amount of injected water is essential to an understanding of the system response as conditions within the gaseous reaction bubble will be controlled by the water inflow rate, especially during the initial period following a break when the reaction rate will have little diffusion dependence. The initial water states can range from subcooled liquid to superheated steam while the conditions within the gaseous reaction bubble can give rise to pressures greater than the water reservoir pressure. Complete specification of heat transfer in the water tubes will not be necessary, and the time-span of greatest interest will be the 100 msec following the initiating event.

The analytical model chosen for calculation of water injection rate assumes homogeneous one-dimensional flow. The governing equations are solved using an explicit finite difference scheme. Two-phase regimes are not treated separately, that is, two-phase effects are seen through the equation of state. This implies that two-phase calculations are based on equal phase velocities and equal phase temperatures (as are many computer codes in present use (for example, Moore and Rettig, 1973) [1]). A discussion of the advantages of this type of solution scheme for blowdown problems is given elsewhere [2].

Results are shown for three different problems. In the first, a comparison is made with the experimental data of Edwards and O'Brien [3] dealing with blowdown from a closed-end pipe with initially subcooled water. This experiment is presently used by the nuclear industry to verify computational models [4]. The second problem involves blowdown of initially two-phase water from a reservoir to a receiver at atmospheric pressure. A comparison is made between these calculated results and those from a current critical flow model (Moody 1975 [5]). The last problem is a study showing the effect of variations in discharge area upon the blowdown of subcooled water.

Mathematical Model

1. Basic Equations

The equations of continuity, momentum, energy, state and wall movement for one-dimensional flow with heat transfer, gradual area change, wall friction and gravity for a homogeneous model of two-phase water may be stated as follows:

Continuity,

$$\frac{\partial \rho}{\partial t} + \frac{\partial}{\partial x}(\rho u) = \frac{\dot{m}}{A} - \frac{\rho}{A}\left(\frac{\partial A}{\partial t} + u\frac{\partial A}{\partial x}\right) \tag{1}$$

Momentum,

$$\frac{\partial}{\partial t}(\rho u) + \frac{\partial}{\partial x}(\rho u^2 + P) = \rho g\cos\theta - \frac{f}{2D}\rho u|u| - \frac{\rho u}{A}\left(\frac{\partial A}{\partial t} + u\frac{\partial A}{\partial x}\right) \tag{2}$$

Energy,

$$\frac{\partial}{\partial t}\left(\rho e + \frac{1}{2}\rho u^2\right) + \frac{\partial}{\partial x}\left(\rho u e + \frac{1}{2}\rho u^3 + Pu\right) = \frac{\rho \dot{q}}{A} - \left(\frac{\rho e + \frac{1}{2}\rho u^2 + P}{A}\right)\left(\frac{\partial A}{\partial t} + u\frac{\partial A}{\partial x}\right) \tag{3}$$

State,

$$P = P(\rho, e) \tag{4}$$

Wall movement,

$$\frac{1}{A}\frac{\partial A}{\partial t} = \frac{D}{hE}\frac{\partial P}{\partial t} \tag{5}$$

After rearrangement, eqs. (1), (2), and (3) may be reduced to the following matrix form

$$\frac{\partial \vec{U}}{\partial t} + \frac{\partial \vec{F}(\vec{U})}{\partial x} = \vec{S}(\vec{U}) \tag{6}$$

where

$$\vec{U} = \begin{Bmatrix} \rho \\ \rho u \\ \rho e + \frac{1}{2}\rho u^2 \end{Bmatrix} \qquad \vec{F}(U) = -\begin{Bmatrix} \rho u \\ \rho u^2 + P \\ \rho u e + \frac{1}{2}\rho u^3 + Pu \end{Bmatrix}$$

$$\vec{S}(\vec{U}) = -\begin{Bmatrix} \rho \\ \rho u \\ \rho e + \frac{1}{2}\rho u^2 - P \end{Bmatrix}\frac{1}{A}\left(\frac{\partial A}{\partial t} + u\frac{\partial A}{\partial x}\right) + \frac{\dot{m}}{A}\begin{Bmatrix} 1 \\ 0 \\ 0 \end{Bmatrix} + \rho\begin{Bmatrix} 0 \\ g\cos\theta - \frac{f}{2D}u|u| \\ \dot{q}/A \end{Bmatrix}$$

2. Finite Difference Method

Equations (6) are now in a conservation-law form, and as such are suitable for solution using the Lax-Wendroff [6] finite difference scheme. The two-step procedure is set up by dividing the pipe into N cells (with N+1 mesh points) as illustrated in fig. 1. The scheme then requires determining $\vec{U}$ at the N cell centers at time $t+\Delta t/2$ in the following manner,

$$\vec{U}^{t+\Delta t/2}_{j+1/2} = \frac{1}{2}(\vec{U}^t_{j+1} + \vec{U}^t_j) - \frac{1}{2}\beta(\vec{F}(\vec{U})^t_{j+1} - \vec{F}(\vec{U})^t_j) + \frac{1}{4}\beta\Delta x(\vec{S}(\vec{U})^t_{j+1} + \vec{S}(\vec{U})^t_j)$$

Having determined $\vec{U}$ at N cells for time $t+\Delta t/2$, the flux vector, $\vec{F}$, and source vector, $\vec{S}$, are determined at these points by using the equation of state. A new vector $\vec{U}$ for the n-1 interior mesh points (at time $t+\Delta t$) may now be determined from the second step as follows,

$$\vec{U}^{t+\Delta t}_j = \vec{U}^t_j - \beta\left(\vec{F}(\vec{U})^{t+\Delta t/2}_{j+1/2} - \vec{F}(\vec{U})^{t+\Delta t/2}_{j-1/2}\right) + \frac{1}{2}\beta\Delta x\left(\vec{S}(\vec{U})^{t+\Delta t/2}_{j+1/2} + \vec{S}(\vec{U})^{t+\Delta t/2}_{j-1/2}\right)$$

where $\beta = \Delta t/\Delta x$ which is directly related to the stability of the numerical scheme. The Courant-Friedricks-Levy stability criteria is

$$\Delta t = \delta \frac{\Delta x}{(c + |u|)_{max}}$$

where δ is a safety reduction factor (namely $0.9 \leq \delta \leq 0.99$).

3. Boundary Conditions

In this finite difference scheme three boundary conditions are available from the definition of the problem. Three computational boundary conditions must be generated as six boundary conditions are needed to solve the finite difference equations. The degree of incompatibility of these new constraints on the problem will have a great effect on the solution of the equations. The larger the degree of incompatibility, the more the solution will be in error (if a stable solution can even be obtained). At the inflow end of the pipe two material boundary conditions were specified, namely,

$$e_o + \frac{P_o}{\rho_o} = e_1 + \frac{P_1}{\rho_1} + \frac{1}{2}\rho_1 u_1^2 \qquad \text{constant total energy}$$

$$S_o = S_1 \qquad \text{isentropic flow}$$

The computational boundary condition was determined from the characteristic formulation of the problem with the negative characteristic being used at the inflow end of the pipe. This equation is

$$P_1 - P_S - (\rho c)_{1S}(u_1 - u_S) = \phi_{1S}\Delta t$$

where ϕ_{1S} is the nonhomogeneous part of the characteristic equation averaged between mesh point "1" (the pipe boundary at the advanced time, $t+\Delta t$) and characteristic point "S" (see fig. 1).

At the outflow boundary only one material boundary condition exists, namely

$$P_e = P_{N+1} + \frac{1}{2}K\rho_{N+1}u^2_{N+1}$$

or $u_{N+1} = c_{N+1}$ if flow is choked.

Again the computational boundary conditions were determined from the characteristic formulation. These two additional constraints are depicted by the positive characteristic equation and the particle path respectively,

$$P_{N+1} - P_R + (\rho c)_{N+1R}(u_{N+1} - u_R) = \phi_{N+1R}\Delta t$$

$$P_{N+1} - P_T - c^2_{N+1T}(\rho_{N+1} - \rho_T) = \phi_{N+1T}\Delta t$$

The three equations at each boundary, in conjunction with the equations of state, are sufficient to determine the necessary boundary conditions.

4. Equation of State

Pressure transients in an LMFBR steam generator will involve water states ranging from subcooled liquid to superheated steam, and include the two phase region. Computation of water properties must be done continuously through all these regimes, and use an efficient computational scheme since millions of calls will be made to water properties routines during execution of a problem.

In the present equation of state, the independent variables are internal energy and specific volume with property values being based upon Keenan's [7] formulation which is valid to 1000 bars and 1300°C. This formulation, which expresses the Helmholtz function in terms of temperature and specific volume, can be used for all single phase water states (liquid and vapor) within the above boundary. Iteration routines are used for independent variables pairs other than temperature and specific volume. This procedure has proven satisfactory in the cases run to date which use values from the previous step as initial values in the iteration routines. Convergence was obtained in all cases to the degree of precision desired.

It is also possible to increase computational speed by use of an alternate scheme. Use is made of the method of "Transfinite Interpolation" [8] to approximate properties in selected regions by the use of blending functions. Typical regions are regions 1 and 2 in fig. 2.

Using the blending functions described in reference [4], a surface representing any equilibrium thermodynamic property may be expressed in the form

$$\begin{aligned} F(Z1,Z2) &= (1-Z1)F(0,Z2) + Z1\,F(1,Z2) + (1-Z2)F(Z1,0) + Z2\,F(Z1,1) \\ &\quad - [(1-Z1)(1-Z2)F(0,0) + (1-Z1)Z2\,F(0,1) + Z1(1-Z2)F(1,0) + Z1\,Z2\,F(1,1)] \end{aligned} \tag{7}$$

where Z1 and Z2 are independent variables in a transformed domain. Z1 and Z2 are taken to vary between zero and one and may be considered to be dummy variables which are implicit functions of e and v.

For example, referring to region 2 of fig. 2 (the superheated vapor region), it is desired to find pressure as a function of internal energy and specific volume. That is, a transformation is sought between the variables (e,v) and (Z1,Z2). The region boundaries are expressed in terms of the dummy parameters (Z1,Z2) as follows:

Table 1. Expressions used to represent internal energy and specific volume at region boundaries

Parameter	u	v	Segment
Z2 = 0	$e(Z1,0) = e_{AD}(Z1)$	$v(Z1,0) = v_A+Z1(v_D-v_A)$	AD
Z2 = 1	$e(Z1,1) = e_{BC}(Z1)$	$v(Z1,1) = v_B+Z1(v_C-v_B)$	BC
Z1 = 0	$e(0,Z2) = e_A+Z_2(e_B-e_A)$	$v(0,Z2) = v_A$	AB
Z1 = 1	$e(1,Z2) = e_D+Z2(e_C-e_D)$	$v(1,Z2) = v_C$	CD

where the correspondence between points is as follows:

Point	
e-v plane	Z1-Z2 plane
A	0,0
B	0,1
C	1,1
D	1,0

Substituting the expressions in Table 1 into eq. (4) gives

$$e(Z1,Z2) = e_{AD}(Z1) + Z2\,(e_{BC}(Z1) - e_{AD}(Z1))$$

and

$$v(Z1,Z2) = v_A + Z1\,(v_C - v_A)$$

or, solving for Z1 and Z2

$$Z1 = (v - v_A)/(v_C - v_A) \tag{8}$$

and

$$Z2 = (e - e_{AD})/(e_{BC} - e_{AD}) \tag{9}$$

Thus, given values of (e,v), eqs. (8) and (9) directly give the corresponding values of (Z1,Z2). Any other property (pressure, entropy, etc.) would then be known from an expression of the form of eq. (7).

In order to use this procedure, values of properties along region boundaries ($e_{BC}(Z1)$, $e_{AD}(Z1)$, etc.) must be provided. The use of cubic splines [9] was found to be well suited to this purpose.

Further details of this surface approximation technique can be found in other references, e.g., [10]

Table 2 gives a comparison between calculations done using this method and using Keenan's formulation.

The size of the region selected for approximate computation should be selected to compromise between precision and range of property values. Fig. 2 shows the parameters defining these regions. The compressed liquid region and superheat region are both specified by high and low values of saturation pressure (PMIN,PSATM), maximum liquid pressure (PMAX), and a maximum vapor temperature (TMAX). In the example above these values were 300 psia, 2450 psia, 3000 psia and 716°F, respectively. In addition, maximum and minimum saturation pressures must be specified (PSMIN,PSMAX).

A check is done by the code to determine whether the input values fall outside the specified regions in which case computation is done using the formulation.

Results

Sample problems were solved using a finite difference subprogram based upon the formulation presented in this paper. Several problems treating single phase (subcooled water or superheated steam) decompression of water were solved and compared to results obtained by other well established methods of solution. In all cases the results obtained by the present code compare very favorably with the results obtained from established methods. These problems served as code verification and did not involve two-phase conditions, hence are not included here.

The results from three sample problems which are believed to be of interest were selected for presentation. The first problem involves the blowdown of subcooled water from a closed pipe where the water flashes into the two-phase regime. The second problem examines the decompression of water initially in the two-phase regime where the reservoir is also in the two-phase regime. The third problem investigates the effects of choking on the decompression of subcooled water.

The first problem, the blowdown of subcooled water from a closed ended pipe is specified so comparisons can be made with the experimental data reported by Edwards, et al. [3] (the so-called standard problem number 1 for Nuclear Industry code verification). The parameters identifying this problem are shown in Table 3 and the geometry seen in fig. 3. Results from three stations are compared with the experimental results and are depicted in fig. 4. The results presented are for the short time history only, since the present code has provisions only for reservoir and receiver type boundary conditions. Therefore, the solution presented is only valid until the reflected wave arrives at the station being examined.

Each of the three stations selected for comparisons indicates that the results produced from the code compare favorably. The only noticeable discrepancy exists between the calculated and measured times of wave front arrivals at the recording stations. Greater agreement in arrival time would result with a time-dependent break opening model rather than the instantaneous model used.

It should be noted that the pressure histories of these three stations compare extremely well, especially if the wave fronts were shifted to coincide and thus negating any initialization or transient errors produced fron either the code assumptions or experimental inaccuracies. It should also be noted that the comparisons reported here are of the same order of accuracy as those calculated by more elaborate codes [4].

The second sample problem treats the blowdown of initially two-phase water through frictionless pipes. Results from the present model are compared with calculations according to a current critical flow model (Moody, 1975 [5]).

As shown on Table 4, the largest difference between the results calculated by this code and the results predicted by Moody is at the exit. The local choking flow model of the code showed a lower exit pressure than did the Moody model. Realizing that a basic difference exists between the analytical models, (Moody's assumes annular flow as opposed to the code's assumption of homogeneous flow) any closer agreement between the results compared in Table 2 should not be expected. The time dependent exit discharge rate is given in fig. 5. Fig. 6 shows the pressure transient at selected points along the pipe.

The last sample problem is a hypothetical problem, the sole purpose is to assess the effect of choking on two-phase decompression of subcooled water. Two problems are solved in which all parameters are identical except for exit losses at flow discharge. In choked flow a value K = 0.05 is used for the loss factor. For non-choked flow a value of K = 0.75 is used. This value indicates a significant flow blockage or area reduction at the exit. Results are shown in figs. 7 and 8. It is interesting to note how localized the effects of choking are, even though the flow characteristics near the exit are seemingly significantly different.

There exists no discernible difference in the results at the pipe midpoint or at the reservoir end of the pipe for the different choices of loss coefficient. This may indicate that the concern over a choking model may be somewhat overstated. Certainly further study on this point is desirable.

Conclusions

The above results show good agreement between the present model and other sources.

Assumptions made in the model must continually be checked for validity as experience is gained with the code. Some of the most important of these are:

(1) one-dimensional flow.

(2) homogeneous flow. Comparisons against models allowing differing liquid and vapor phase velocities with transport between phases [11,12] must be made.

(3) Thermodynamic equilibrium. The code calculates local values of internal energy and specific volume, then uses these values in an equation of state to determine all other water properties. As the equation of state is based upon equilibrium data, attention must be paid to deviations from equilibrium.

(4) Sonic flow. The code presently uses local properties to calculate a sonic speed at each point assuming no mass transfer between phases and each phase able to vary isentropically independent of saturation constraints [13]. The maximum flow rate (at the exit) is not allowed to exceed the choked flow condition.

Although continued examination of the modeling assumptions will be necessary as wider application of this code is made, the present simplified model appears to offer good agreement with theory and experiment while providing a solution scheme applicable over a wide range of problems.

References

[1] MOORE, K. V., and RETTIG, W. H., "Relap4 - A Computer Program for Transient Thermal-Hydraulic Analysis," ANCR-1127, Dec. 1973, Aerojet Nuclear Co., Idaho Falls, Idaho.

[2] LYCZKOWSKI, R. W., GRIMESEY, R. A., and SOLBRIG, C. W., "Pipe Blowdown Analyses using Explicit Numerical Schemes," 15th National Heat Transfer Conference, August 1975.

[3] EDWARDS, A. R., and O'BRIEN, T. P., "Studies of Phenomena Connected with the Depressurization of Water Reactors," J. BNES, 9, 125-135, 1970.

[4] SAWTELLE, G. R., et al., "Comparison of Relap4 Predictions with Standard Problems 1, 2, and 3," EPRI NP-205.

[5] MOODY, F. S., "Maximum Discharge Rate of Liquid-Vapor Mixtures from Vessels," Non-Equilibrium Two-Phase Flows, ASME, New York, 1975, pp. 27-36.

[6] LAX, P., and WENDROFF, B., "System of Conservation Laws," Ann. Pure and Applied Math., Vol. XII, 1960.

[7] KEENAN, J. H., KEYES, F. G., HILL, P. G., and MOORE, J. G., "Steam Tables," John Wiley and Sons, New York, 1969.

[8] HALL, C. A., and MUTAFELIJA, B. A., "Transfinite Interpolation of Steam Tables," J. Computational Physics, 10, 79-91, 1975.

[9] AHLBERG, J. H., NILSON, E. N., and WALSH, J. L., "The Theory of Splines and Their Applications," Mathematics in Science and Engineering, 38, Academic Press, New York, 1967.

[10] GORDON, W. J., and HALL, C. A., Num. Math. 17, 1973.

[11] HUGHES, E. D., LYCZKOWSKI, R. W., and MCFADDEN, J. H., "An Evaluation of State-of-the-Art Two-velocity Two-phase Flow Models and their Applicability to Nuclear Reactor Transient Analysis, EPRI NP-143, TSA 75-317, Final Report, February 1976.

[12] STUHMILLER, J. H., "The Application of Two-phase Flow Modeling," EPRI NP-349, Project 599, Final Report, January 1977.

[13] DAVIES, A. L., "The Speed of Sound in Mixtures of Water and Steam," EURATOM Report, Proceedings Symposium on Two-Phase Flow Dynamics at Eindhoven, 1967.

Work performed under the auspices of the U. S. Energy Research and Development Administration.

Table 2. Pressure in Superheat Region Calculated by Interpolation Compared with Keenan's Formulation

Pressure (psia)

Z1 \ Z2	0		.2		.4		.6		.8		1.0	
	Interp.	Form.	Interp.	Form.	Interp.	Form.	Interp.	Form.	Interp.	Form.	Interp.	Form.
0	432.93	432.93	406.45	406.45	379.78	379.78	353.04	353.04	326.40	326.40	300.00	299.99
.2	643.30	643.30	605.75	606.17	568.38	568.94	531.30	531.80	494.64	494.94	458.50	458.50
.4	942.45	942.45	890.83	891.37	839.77	840.46	789.36	789.95	739.68	740.02	690.80	690.80
.6	1350.21	1350.21	1282.06	1282.33	1214.87	1215.15	1148.67	1148.87	1083.53	1083.62	1019.46	1019.46
.8	1867.79	1867.79	1783.48	1783.31	1700.49	1700.19	1618.87	1618.53	1538.61	1538.38	1459.71	1459.72
1.0	2449.66	2449.66	2356.33	2356.33	2264.70	2264.71	2174.80	2174.80	2086.58	2086.58	1999.99	2000.00

Table 3. Adjusted Initial Temperatures for Standard Problem 1

Location	Tadj (°F)	Distance From Leak, ft
GS-1	437	0.55
GS-2	436	1.07
GS-3	450	3.81
GS-4	447.5	6.80
GS-5	450	8.62
GS-6	452.5	10.44
GS-7	447.5	13.18

Table 4. Comparison - Code Prediction vs. Moody

	Present Calc.	Moody's Crit. Flow	% Diff.
Inlet Stag. Enthalpy (Btu/lbm)	782.35	782.35	0
Exit Stag. Enthalpy (Btu/lbm)	740.50	782.35	8.7
Inlet Pressure (psia)	1740	1560	10.2
Exit Pressure (psia)	1100	1600	31.2
Exit Quality (%)	22	28	21.4
Max. Discharge Rate ($lbm/sec \cdot ft^2$)	8440	10,000	15.6

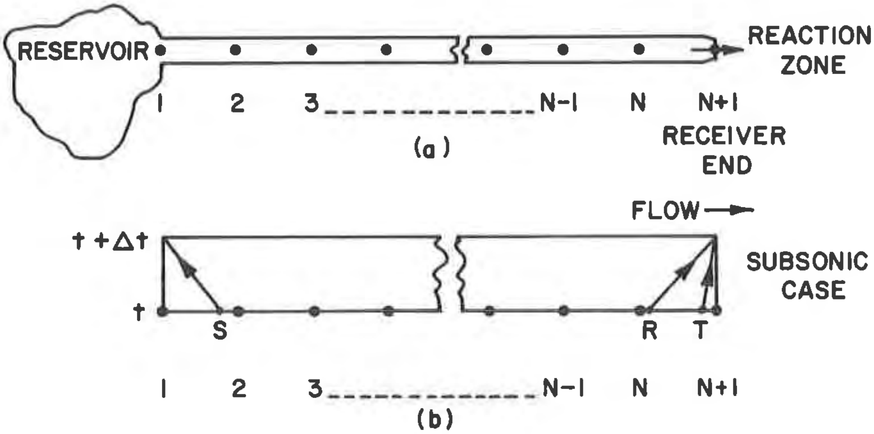

1 Finite difference model

a) Pipe divided into N equal parts

b) Model showing characteristic points in boundary cells

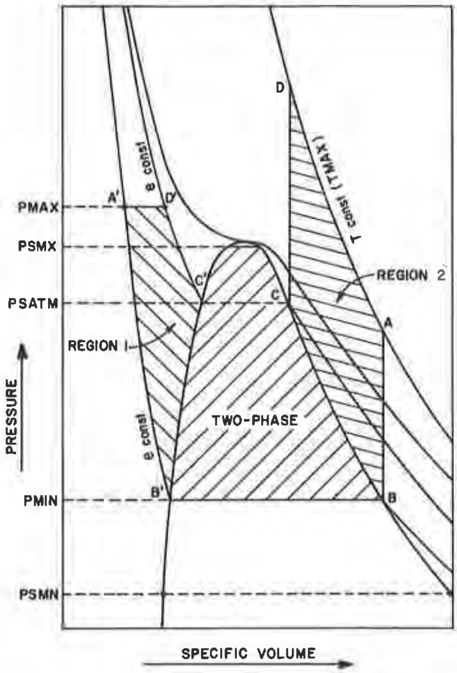

2 Variables necessary to specify regions for interpolation of water properties

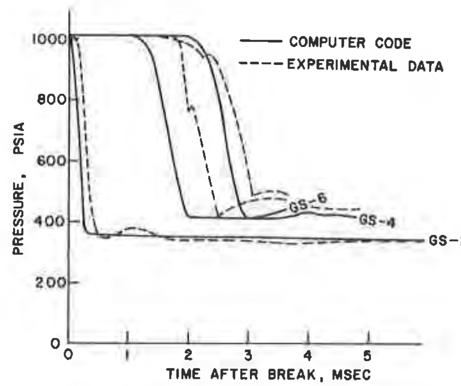

3 General dimensions for standard problem number one

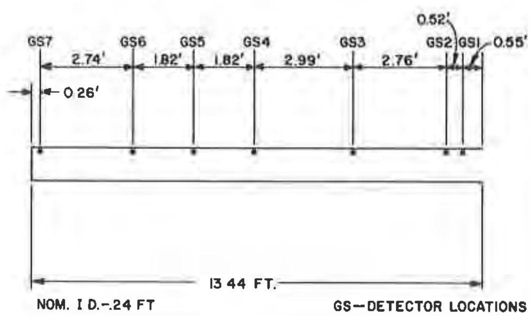

4 Pressure histories for standard problem number one

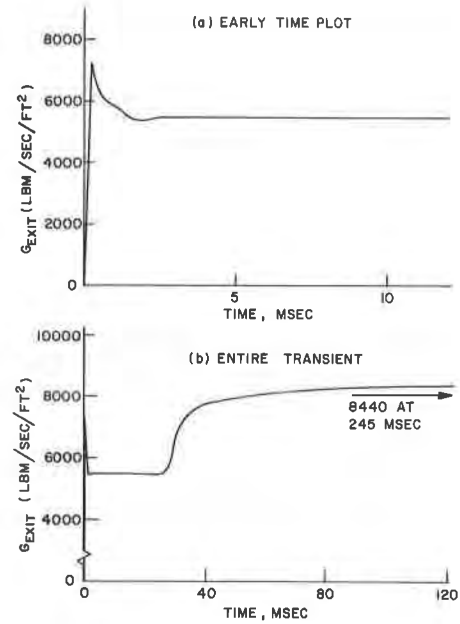

5 Transient mass flow rate for two-phase blowdown

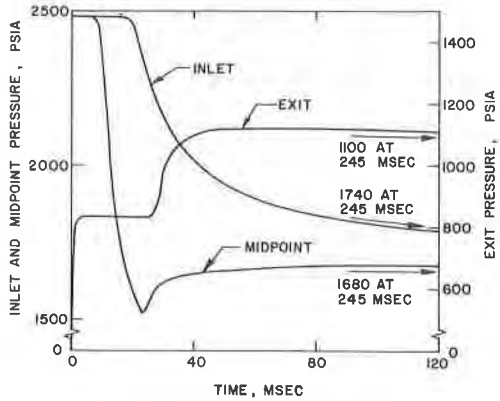

6 Pressure transients for two-phase blowdown

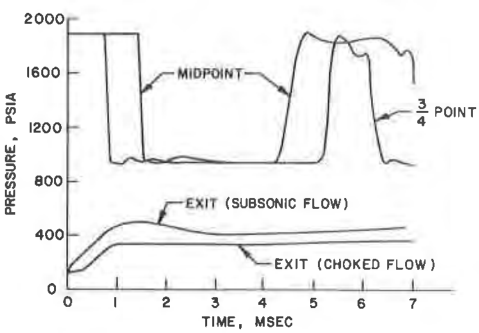

7 Pressure transients comparing choked and unchoked flow

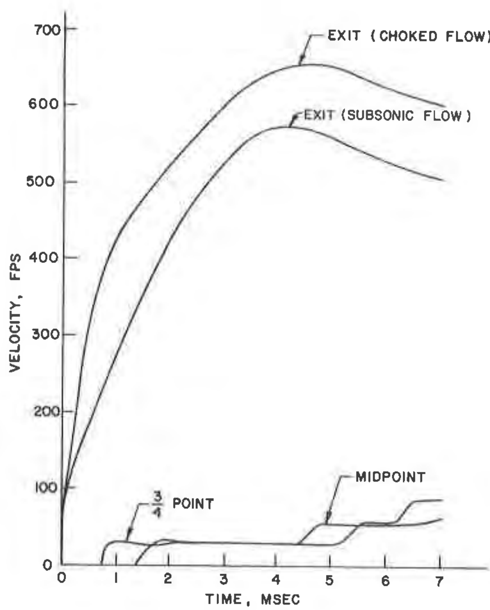

8 Velocity transients comparing choked and unchoked flow